Biosensors and Bioelectronics 24 (2008) 222–227

Contents lists available at ScienceDirect

Biosensors and Bioelectronics

journal homepage: www.elsevier.com/locate/bios

A third-generation hydrogen peroxide biosensor based on horseradish peroxidase immobilized in a tetrathiafulvalene–tetracyanoquinodimethane/multiwalled carbon nanotubes film

Zhijun Cao, Xueqin Jiang, Qingji Xie*, Shouzhuo Yao

Key Laboratory of Chemical Biology & Traditional Chinese Medicine Research (Ministry of Education of China), College of Chemistry and Chemical Engineering, Hunan Normal University, Changsha 410081, China

ARTICLE INFO

Article history:
Received 24 January 2008
Received in revised form 23 March 2008
Accepted 25 March 2008
Available online 29 March 2008

Keywords:
Horseradish peroxidase (HRP)
Tetrathiafulvalene–tetracyanoquinodimethane (TTF–TCNQ)
Multiwalled carbon nanotubes (MWCNTs)
Amperometric H_2O_2 sensor
Enzymatic specific activity

ABSTRACT

A new third-generation biosensor for H_2O_2 assay was developed on the basis of the immobilization of horseradish peroxidase (HRP) in a nanocomposite film of tetrathiafulvalene–tetracyanoquinodimethane (TTF–TCNQ)/multiwalled carbon nanotubes (MWCNTs) modified gold electrode. The prepared HRP/TTF–TCNQ/MWCNTs/Au electrode was used for the bioelectrocatalytic reduction of H_2O_2, with a linear range from 0.005 to 1.05 mM and a detection limit of 0.5 μM for amperometric sensing of H_2O_2. In addition, a novel method on the basis of electrochemical quartz crystal microbalance (EQCM) measurements was proposed to determine the effective enzymatic specific activity (ESA) of the immobilized HRP for the first time, and the ESA was found to be greater at the TTF–TCNQ/MWCNTs/Au electrode than that at the MWCNTs/Au or TTF–TCNQ/Au electrode, indicating that the TTF–TCNQ/MWCNTs film is a good HRP-immobilization matrix to achieve the direct electron transfer between the enzyme and the electrode.

1. Introduction

It is interesting and important to design the mediator-free third-generation enzyme electrodes, featured by a direct electron transfer between enzymes and the conjoint electrodes, for the detection of chemical/biological molecules (Di et al., 2004; Khan et al., 1996; Koopal et al., 1992; Os et al., 1996; Ren et al., 2005; Song et al., 2006; Stoica et al., 2006; Tang et al., 2006; Wang, 2008; Zhao et al., 2005). However, the direct electron communication between the redox center of the immobilized enzymes and the electrode is often shielded by the insulating outer protein shell (Yabuki et al., 1989). Therefore, it is necessary to discover a specific conducting material that can connect the active center of redox enzymes with the electrode surface, or develop a special electrode that can directly reach into the active center of enzymes. There have been a lot of publications reporting special materials for the modification of electrode surface to achieve a direct electron transfer between enzymes and the electrodes, of which nanoparticles (Bartlett et al., 1992; Heller, 1992; Xu and Han, 2004), conducting polymers (Koopal et al., 1992; Razola et al., 2002), DNA (Song et al., 2006) and organic conducting salts (Palmisano et al., 2002; Khan et al., 1996) are good examples. However, little attention has been paid to the quantitative measurement and description of the relationship between the direct electron communication and the enzymatic activity of the immobilized enzyme. Very recently, with the electrochemical quartz crystal microbalance (EQCM) technique, Su et al. (2008) measured the electroactivity of sodium dodecyl benzene sulfonate (SDBS)-treated glucose oxidase (GOD) adsorbed on a multiwalled nanotubes (MWCNTs)/Au electrode as a function of the enzymatic specific activity (ESA, defined as the enzymatic activity per unit mass of enzyme) of the adsorbed GOD, and found that the electroactivity and the ESA of the immobilized GOD responded oppositely to the presence of MWCNTs and SDBS, and the portion of the adsorbed GOD showing electrochemical activity exhibited almost no enzymatic activity.

Tetrathiafulvalene–tetracyanoquinodimethane (TTF–TCNQ), a typical organic charge-transfer complex (CTC), has been used as an ideal material for the modification of electrode surfaces due to its insolubility in water, decent conductivity at room temperature, and easy-shaping in its crystal sizes and form. It was utilized to oxidize a variety of flavoproteins in the early days (Albery et al., 1985, 1987; Cenas and Kulys, 1981; Freund and Brajter-Toth,

* Corresponding author. Tel.: +86 731 8865515; fax: +86 731 8865515.
E-mail address: xieqj@hunnu.edu.cn (Q. Xie).

0956-5663/$ – see front matter © 2008 Elsevier B.V. All rights reserved.
doi:10.1016/j.bios.2008.03.021

1989; Hill et al., 1988) and later to immobilize a variety of redox enzymes on electrode surfaces, including xanthine oxidase (Korell and Spichiger, 1993), glucose oxidase (Palmisano et al., 2002; Khan et al., 1996) and peroxidase (Korell and Spichiger, 1994), though the exact redox mechanism of the related enzymes on the electrode surfaces is still a controversy. Cenas and Kulys (1981) have suggested a dissolved component of the organic electric salts (NMP-TCNQ) to serve as an electron mediator in the oxidation process of glucose oxidase, but Albery et al. (1985) and Hill et al. (1988) proposed that a heterogeneous electron transfer could directly take place between enzymes and the conjoint electrodes. Freund and Brajter-Toth (1989) have suggested that the electrochemical kinetics of TTF–TCNQ electrodes can be controlled by manipulating their surface structure, and in certain cases, the electrode can behave like arrays of ultramicroelectrodes. Furthermore, Khan et al. (1996) suggested that variation of CTC components, methods of CTC preparation and electrode fabrication, experimental conditions, and especially applied potentials, greatly affected the oxidation mechanism of enzymes, and they developed a novel approach to make a stable metal-like CTC on a flexible and electrochemical inert polymer film for the direct oxidation of glucose oxidase.

Much attention has also been paid to carbon nanotubes (CNTs) for the development of biosensors in the past decades, among which the application of nanocomposite materials through the integration of CNTs with various bio-macromolecules, conductive polymers, or other metal-nanoparticles is the most remarkable one. By this means, the carbon nanocomposite materials are endowed with unique features for the immobilization of enzymes on the surface of various sensors. Many nanocomposite materials have been developed and applied to construct biosensors, such as MWCNTs/chitosan (Qian and Yang, 2006; Zhou et al., 2007), polyaniline/MWCNTs (Luo et al., 2006), sol–gel-derived ceramic-MWCNTs nanocomposite (Chen and Dong, 2007), Au–Pt alloy nanoparticles/MWCNTs (Kang et al., 2007). However, to our knowledge, the CTC/CNTs nanocomposite film is not examined as an enzyme-immobilization matrix to date.

In this study, a new TTF–TCNQ/MWCNTs nanocomposite film is proposed to immobilize horseradish peroxidase (HRP), and a third-generation H_2O_2 biosensor with good performance is thus fabricated. Also, the EQCM method is proposed to determine the effective ESA of the immobilized HRP.

2. Experimental

2.1. Chemicals

HRP (E.C.1.11.1.7, 250 U mg^{-1}) was purchased from Sinopharm Chemical Reagent Co., Ltd. TTF and TCNQ were purchased from Aldrich and used without further purification. A 30% H_2O_2 solution was purchased from Shanghai Taopu Chemical Factory, and a fresh solution of H_2O_2 was prepared daily. Acetonitrile (ACN, guaranteed reagent) was purchased from Jiangsu Hanbon Sci. & Tech. Co. Ltd. *N*,*N*-dimethylformamide (DMF, AR) and tetrahydrofuran (THF, AR), 4-Amino-antipyrine (AR) and phenol (AR) were obtained from Shanghai Shangpu Chemicals Factory. MWCNTs (~20 nm in diameter) were purchased from Shenzhen NanoPort Ltd., China. Gelatin (Gel) was purchased from Sigma. Phosphate buffer solution (PBS) (50.0 mM K_2HPO_4–KH_2PO_4 + 0.100 M K_2SO_4) was used as the supporting electrolyte, and its pH value was adjusted to 7.0 (monitored with a PHS-3C pH meter, Leici, China), unless otherwise specified. All other chemicals were of analytical grade. All solutions were prepared using double-distilled water. All experiments were performed at room temperature round at 20 °C.

2.2. Apparatus

All electrochemical experiments were performed on a CHI660A electrochemical workstation (CH Instruments Co., USA) controlled by the CHI660A software. A research QCM (Maxtek Inc., USA) with a crystal measurement card (5.1–10 MHz) controlled by the Maxtek software, was used to record the resonant frequency (f_0) and the motional resistance (R_1) data of the resonating quartz crystals, and the readout was comparable with those obtained from an HP4395A impedance analyzer (Zhou et al., 2000). AT-cut piezoelectric quartz crystals (PQCs) with a nominal frequency of 9 MHz and Au electrodes of a 0.6-cm diameter were used. The electrode on one side of PQC was exposed to the solution and served as the working electrode (WE), while that on the other side faced air. A platinum foil served as the counter electrode. A KCl-saturated calomel electrode (SCE) served as the reference electrode, and all potentials here were reported versus it. Scanning electron microscopy (SEM) pictures were collected on a JSM 6360-LV scanning electron microscope (JEOL, Japan). The UV–vis absorption spectra were collected on a TU-1221 UV–vis recording spectrophotometer (Beijing Puxi General Instruments Co., China).

2.3. Fabrication of the sensor

Briefly, the MWCNTs were spread and dried on a gold electrode to provide a matrix for the later growth of the TTF–TCNQ CTC crystals, followed by HRP adsorption, gelatin coating and then glutaraldehyde cross-linking. The detailed process for the sensor fabrication is described as follows. In the first step, the gold electrode surface was treated generally by washing with $H_2SO_4 + H_2O_2$ (v/v, 3:1) for 1 min and then with double-distilled water. The gold electrode was subject to potential cycling (0–1.5 V, 50 mV s^{-1}) in 0.200 M $HClO_4$ for sufficient cycles to obtain reproducible cyclic voltammograms. The gold electrode was washed with double-distilled water and dried under an infrared light. In the second step, a certain amount of the MWCNTs solution dispersed by DMF was spread on the gold electrode, and dried at room temperature, then washed with double-distilled water. After drying it again at room temperature, a stable MWCNTs/Au electrode was achieved. In the third step, the TTF–TCNQ crystals were in situ grown by a two-step procedure. Firstly, 2.00 μL of a TCNQ solution (2.00 g L^{-1} in THF) was cast on the MWCNTs/Au layer and dried for a few minutes, then 2.00 μL of a TTF solution (2.00 g L^{-1} in ACN) was slowly spread over the last TCNQ cast. The complete casting procedure (both TCNQ and TTF steps) was repeated different times in order to get various amounts of TTF–TCNQ modifications. After the CTC's crystallization had been completed, the electrode was gently washed with ACN and then with diethyl ether to scour the unreacted species off. The mass of TTF–TCNQ (Δm in mg) on the electrode was measured by the "dry" frequency shift in air, as depicted by the Sauerbrey equation (Buttry and Ward, 1992).

$$\Delta m = \frac{4.417 \times 10^8 \Delta f_{0d} A}{f_{0g}^2} \quad (1)$$

where A in cm^2 is the piezoelectrically active electrode area exposed to the solution, f_{0g} in Hz is the nominal frequency of the AT-cut PQC, and Δf_{0d} ($\Delta f_{0d} = f_{0d1} - f_{0d2}$, f_{0d2} and f_{0d1} are the "dry" resonant frequencies in air after and before the modification, respectively) in Hz is the frequency response.

The HRP immobilization proceeded in two steps. In the first step, an excess amount of HRP solution (20.0 g L^{-1} HRP in water) was spread over the TTF–TCNQ/MWCNTs/Au electrode and kept in 4 °C refrigeratory for 1 h. The excess HRP solution was then gently removed with filter paper, and the HRP-immobilized electrode was

dried at room temperature, and the amount of the immobilized HRP was measured by the related "dry" frequency shift too. In the second step, 5.00 μL of gelatin (5% gelatin in water, incubated for 30 min at 37 °C before use) was spread uniformly over the surface of the HRP-immobilized electrode, which was kept at room temperature for drying. The gelatin-cast film was then dipped into a glutaraldehyde solution (5% in water) for 60 s, then thoroughly washed with plenty of double-distilled water, and dried at room temperature for several hours. When not in use, the sensor was stored as a dry film in a closed glass bottle at 4 °C. The Gel/TTF–TCNQ/MWCNTs/Au electrode was similarly prepared but without steps of the enzyme modification and the glutaraldehyde cross-linking. Amperometric sensing experiments of the enzyme electrode were accomplished in stirred solutions.

2.4. Estimation of the ESA values

According to the conventional enzymatic activity concept, 1 U of HRP activity (1 U) is defined as the enzymatic consumption of 1 μmol H_2O_2 in 60 s. The effective ESA here is defined as the enzymatic activity in U per unit mass of enzyme (U mg^{-1}),

$$\mathrm{ESA} = \frac{n_{H_2O_2}}{m_{\mathrm{HRP}}} \tag{2}$$

where $n_{H_2O_2}$ (in μmol) is the consumed molar quantity of H_2O_2 in the 60-s enzymatic reaction, m_{HRP} (in mg) is the mass of HRP.

For the immobilized HRP, the EQCM method was proposed to determine its effective ESA here, in which the enzymatically consumed H_2O_2 and mass of immobilized HRP were quantified from chronocoulometry and QCM frequency, respectively. Briefly, the mass of the immobilized HRP (m_{HRP} in mg) was quantified from the dry frequency shift (Δf_{0d}) due to HRP load according to the Sauerbrey equation (Eq. (1)). The amount of consumed H_2O_2 ($n_{H_2O_2}$ in μmol) was obtained from the cathodic charge (Q in μC, 0 V) on the enzyme electrode in the 60-s electrocatalytic reduction of H_2O_2 at saturated concentration. So the effective ESA of the immobilized HRP here ($\mathrm{ESA_Q}$) can be expressed as,

$$\mathrm{ESA_Q} = \frac{Qf_{0g}^2}{4.417 \times 10^8 \times zFA\,\Delta f_{0d}} \tag{3}$$

where $\mathrm{ESA_Q}$ is the ESA (U mg^{-1}) based on EQCM measurements, F is the Faraday constant (96485.33 C mol^{-1}), z is the number of electrons transferred in the related process, Δf_{0d}, A, and f_{0g} are of the same meanings as in Eq. (1).

Conventional UV–vis spectrophotometry was also used to measure the enzymatic activity of the immobilized HRP on the modified electrode (Decker, 1977; Su et al., 2008). The detailed process is given as follows. The enzyme electrode was inserted into a 3 mL stirred PBS (pH 7.0) solution containing 2.5 mM 4-amino-antipyrine and 170 mM phenol, 2 mM H_2O_2, and every 60 s the reaction was stopped by taking the electrode out of the reaction solution, and a stable increase in absorbance at 510 nm due to the oxidation of 4-amino-antipyrine by H_2O_2 through HRP catalysis was recorded. Therefore, the $\mathrm{ESA_{UV}}$ can be expressed as,

$$\mathrm{ESA_{UV}} = \frac{3 \times E_{510} f_{0g}^2}{6.58 \times 4.417 \times 10^8 A\,\Delta f_{0d}} \tag{4}$$

where $\mathrm{ESA_{UV}}$ is the ESA (U mg^{-1}) from conventional UV–vis spectrophotometry, E_{510} is the increase in absorbance at 510 nm in 60 s, 3 is the whole reaction volume (in mL), 6.58 means that 1 U of enzymatic activity can elevate 6.58 in absorbance in 60 s, Δf_{0d}, A, and f_{0g} are of the same meanings as in Eq. (1).

3. Results and discussion

3.1. Electrochemical behaviors of TTF–TCNQ/MWCNTs/Au electrode in pH 7.0 PBS

The electrochemistry of TTF–TCNQ crystals grown on conventional electrodes has been studied previously (Bartlett and Tong, 1997; Freund et al., 1990; Jaeger and Bard, 1979, 1980). In this work, the electrochemical behavior of the Gel/TTF–TCNQ/MWCNTs/Au electrode was characterized by cyclic voltammetry in PBS (pH 7.0). As shown in Fig. 1, the modified electrode exhibited a stable potential region from −0.2 to 0.4 V (curve a). A potential beyond the stable region in the positive direction led to the oxidation of TTF–TCNQ itself, as shown in Fig. 1 (curve b), which started at about 0.4 V and damaged the TTF–TCNQ crystals by forming TTF^{2+} and TCNQ (s). Then by reversing the scanning potential, a cathodic peak was observed at −0.03 V, corresponding to the conversion of TCNQ (s) to insoluble KTCNQ (s). An oxidation peak newly occurred at 0.24 V when the scanning potential was positively scanned again, indicating the oxidation of the KTCNQ (s). Even the positive potential limit was negatively shifted to 0.35 V, the Gel/TTF–TCNQ/MWCNTs/Au

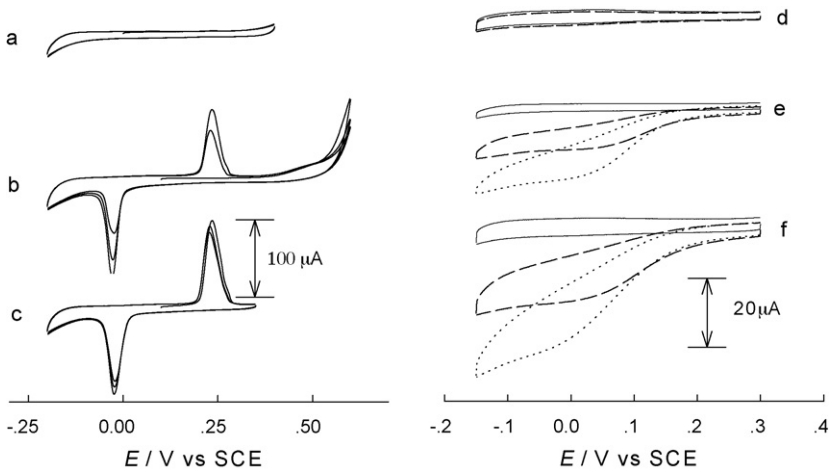

Fig. 1. Cyclic voltammograms for Gel/TTF–TCNQ/MWCNTs/Au (curves a–c), Gel/HRP/MWCNTs/Au (curves d, HRP: 5.30 μg, MWCNTs: 7.4 μg), Gel/HRP/TTF–TCNQ/Au (curves e, HRP: 18.6 μg, TTF–TCNQ: 16.6 μg), and Gel/HRP/TTF–TCNQ/MWCNTs/Au (curves f, HRP: 21.4 μg, MWCNTs: 5.80 μg, TTF–TCNQ: 18.1 μg) in 50.0 mM PBS of pH 7.0 in the absence (solid curves) and presence of 0.500 (broken curves) or 1.00 (dashed curves) mM H_2O_2. Scan rate: 20 mV s^{-1}.

Table 1
The mass and ESA of HRP immobilized on matrices of TTF–TCNQ, MWCNTs, TTF–TCNQ/MWCNTs

	TTF–TCNQ: 16.6 μg	MWCNTs: 7.4 μg	TTF–TCNQ/MWCNTs: 18.1 μg/5.8 μg
Mass of HRP (μg)	18.6	5.3	21.4
Q (mC, 0 V for 60 s)	1.24 ± 0.04	0.0138 ± 0.008	2.16 ± 0.07
ESA_Q (U mg^{-1})	0.34 ± 0.01	0.013 ± 0.008	0.52 ± 0.02
ESA_{UV} (U mg^{-1})	2.1 ± 0.08	2.8 ± 0.07	2.6 ± 0.09

All ESA measurements of the enzyme electrodes were repeated three times and the results are expressed as mean ± S.D.

electrode after the over-oxidation damage of the TTF–TCNQ crystals still exhibited a cathodic peak at about −0.03 V and an anodic peak at 0.24 V with equivalent heights, as shown in Fig. 1 (curve c). The two current peaks can be assigned to the KTCNQ/TCNQ redox couple with the following electrode reaction (Jaeger and Bard, 1979, 1980),

$$KTCNQ(s) \rightleftharpoons TCNQ + K^+ + e^- \quad (5)$$

3.2. Cyclic voltammograms of various modified electrodes in the absence or presence of H_2O_2

The electrochemical performances of Gel/HRP/MWCNTs/Au (sensor I), Gel/HRP/TTF–TCNQ/Au (sensor II) and Gel/HRP/TTF–TCNQ/MWCNTs/Au (sensor III) for detecting H_2O_2 were investigated by cyclic voltammetry in PBS (pH 7.0), and the results are shown in Fig. 1 (curves d, e and f for sensors I, II and III, respectively). In the absence of H_2O_2, much greater non-Faradaic background currents were observed for sensor III, indicating an enhanced surface area of this electrode.

In the presence of H_2O_2, the increase of the reduction current on sensor I was insignificant, but evident reduction currents that are positively correlated with the concentration of H_2O_2 were observed on sensors II and III. The reduction currents were significantly higher on sensor III than those on sensor II at an identical concentration of H_2O_2. The findings should suggest that the presence of TTF–TCNQ crystals and especially the synergetic effects of MWCNTs and TTF–TCNQ crystals largely promoted the HRP-catalyzed reduction of H_2O_2. We calculated the ESA values of HRP on these sensors by the EQCM technique (ESA_Q) and the conventional UV–vis spectrophotometry (ESA_{UV}), and the results are given in Table 1. One can see that the amount of HRP immobilized on the TTF–TCNQ/MWCNTs nanocomposite film was slightly increased in comparison with that on the TTF–TCNQ electrode, and the values of ESA_{UV} for the three sensors showed little difference. In contrast, the ESA_Q of immobilized HRP was much higher on the TTF–TCNQ/Au electrode, especially on the TTF–TCNQ/MWCNTs/Au electrode, compared with the MWCNTs/Au electrode, indicating that the TTF–TCNQ is a better vehicle for electron transfer between HRP and the electrode than the MWCNTs under our experimental conditions. We may assume that the good electrocatalytic reduction of H_2O_2 at 0 V be ascribed to the presence of TTF–TCNQ crystals, which can bridge the activity center of HRP to the electrode and result in the direct electron transfer between HRP and the electrode (Freund and Brajter-Toth, 1989; Khan et al., 1996), as described in Eqs. (6)–(8) (Gorton et al., 1992),

$$HRP(Red) + H_2O_2 \rightarrow HRP(Compound\ I) + 2H_2O \quad (6)$$

$$HRP(Compound\ I) + e^- + H^+ \rightarrow HRP(Compound\ II) \quad (7)$$

$$HRP(Compound\ II) + e^- + H^+ \rightarrow HRP(Red) \quad (8)$$

where HRP (red) is the ferric form of HRP, HRP (compound I) is the oxidized product of HRP, and HRP (compound II) is the intermediate form of HRP.

The values of ESA_Q measured by the EQCM technique are lower than values of ESA_{UV} by conventional UV–vis spectrophotometry, indicating that only part of immobilized HRP could directly communicate electrons with the electrode. The MWCNTs, as a matrix of the growth of TTF–TCNQ crystals, might improve the dispersion of and increase the number of TTF–TCNQ crystals, and enhance the direct electron communication between the immobilized HRP and the electrode for the catalytic reduction of H_2O_2.

SEM pictures for several surfaces are shown in Fig. 2. The MWCNTs were well distributed on the Au electrode, and the TTF–TCNQ crystals on the bare Au electrode were vimineous, and the vimineous CTC crystals appeared to become smaller in diameter on the MWCNTs/Au surface, implying that the modification of MWCNTs on the Au electrode can be in favor of the growth of small-sized tress-like TTF–TCNQ crystals and thus increase the electrode-surface area.

3.3. Effects of experimental conditions

The effect of the amount of loaded TTF–TCNQ was examined (Fig. 3). The amount of immobilized HRP was positively correlated with the amount of the loaded TTF–TCNQ, and the H_2O_2-reduction current was also increased with the increase of the loaded TTF–TCNQ. However, when the load of TTF–TCNQ was over 43.8 μg, the current response increased slightly, though more HRP molecules were immobilized. It seems that an over-loading of the TTF–TCNQ crystals brought about a difficulty for enzyme's active center to communicate with the electrode, and was also unfavorable for the diffusion of the substrate. So it is unnecessary to further increase the amount of loaded TTF–TCNQ beyond 43.8 μg, for the construction of the sensor.

The effect of the amount of loaded MWCNTs was also examined (Fig. 4), the H_2O_2-reduction current was enhanced with the increase of the amount of loaded MWCNTs. While the amount of loaded MWCNTs was over 10.6 μg, the current response exhibited a decreasing decline instead. We think that too much loading

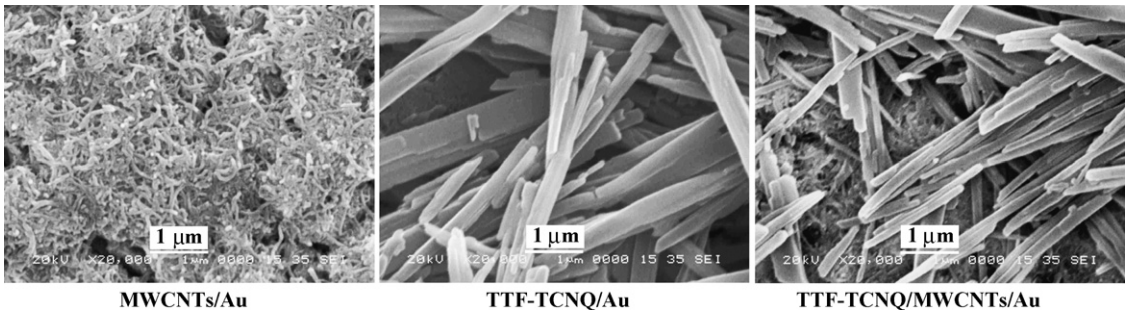

Fig. 2. SEM photographs of several electrode surfaces.

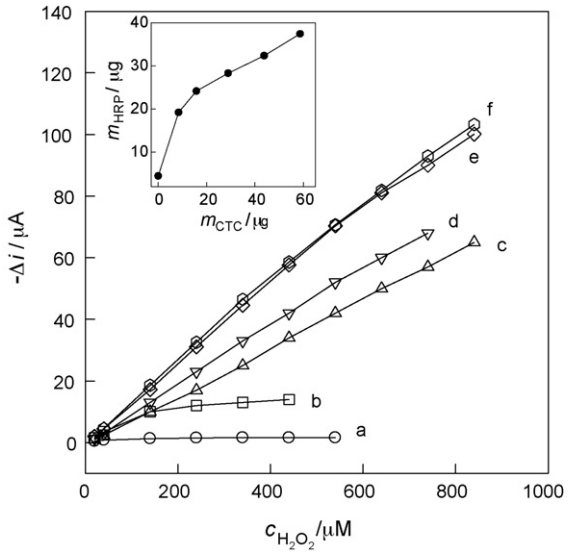

Fig. 3. Effect of the load of TTF–TCNQ on the current response for H_2O_2 reduction at Gel/HRP/TTF–TCNQ/MWCNTs/Au electrodes. TTF–TCNQ: 0 μg (a), 8.40 μg (b), 15.8 μg (c), 28.9 μg (d), 43.8 μg (e), and 58.7 μg (f). MWCNTs: 10.6 μg. Polarization potential: 0 V. Insert shows plot of the load of immobilized HRP versus the load of TTF–TCNQ.

of the MWCNTs may induce thicker MWCNTs stacks on the electrode, which was probably profitless for the growth of CTC crystals but increased the electrode resistance (versus Au), resulting in an adverse effect on the sensor's response. So the amount of loaded MWCNTs should be controlled no more than 10.6 μg here.

The working potential for H_2O_2 sensing was examined in the CTC-stabilized range. We found that the negative-going of the working potential increased the steady-state current (Fig. 1S in the Supplementary Data), where the increasing rate for 1.00 mM H_2O_2 was notably larger than that for 5.00 μM H_2O_2, which is a typical potential-current behavior when direct electron transfer occurs between the electrode and the interfaced redox proteins (Khan et al., 1992, 1996). In this work, 0 V was selected after an overall consideration of the detection sensitivity and film stability.

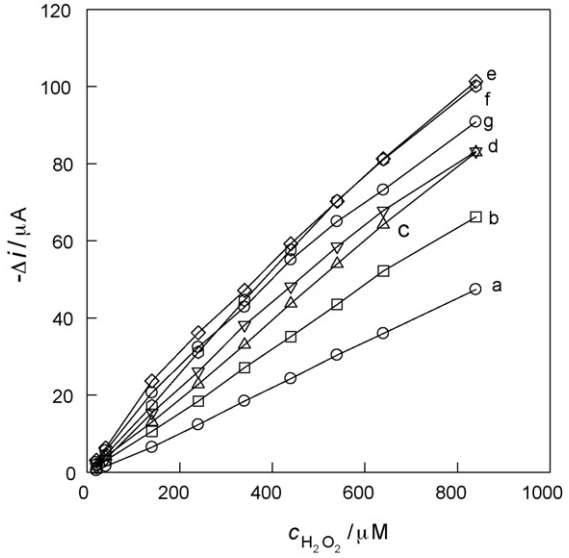

Fig. 4. Effect of the load of MWCNTs on the current response for H_2O_2 reduction at Gel/HRP/TTF–TCNQ/MWCNTs/Au electrodes. MWCNTs: 0 μg (a), 0.50 μg (b), 1.1 μg (c), 4.2 μg (d), 10.6 μg (e), 16.9 μg (f), and 23.2 μg (g). TTF–TCNQ: 43.8 μg. Polarization potential: 0 V.

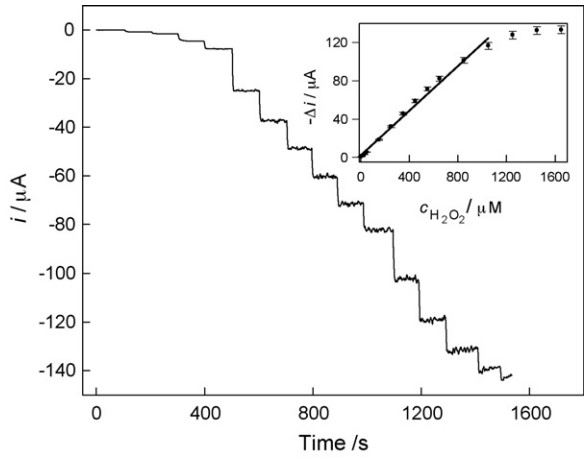

Fig. 5. The chronoamperometric responses to H_2O_2 additions obtained in 50.0 mM PBS (pH 7.0) at a Gel/HRP/TTF–TCNQ/MWCNTs/Au electrode (TTF–TCNQ: 43.8 μg, MWCNTs: 10.6 μg). Potential applied: 0 V. Inset shows the calibration curve.

The pH value of the buffer solution could affect the behavior of H_2O_2 sensor (Fig. 2S in the Supplementary Data). The steady-state current was monotonously increased from 7.8 to 5.7, being consistent with a previous report (Song et al., 2006). Since many HRP-based H_2O_2 sensors were developed for assay under normal physiological circumstances, we suggest a PBS buffer solution with pH value of 7.0 here.

3.4. Amperometric response and enzymatic kinetic parameter

The calibration curve under optimal conditions is shown in Fig. 5. The current response of the enzyme electrode increased linearly with the increase of H_2O_2 concentration from 5.0 μM to 1.05 mM, with a slope of 0.383 A cm^2 M^{-1} (0.295 cm^2 electrode area here) and a linearity correlation coefficient of 0.995, as well as a detection limit of 0.5 μM (3σ), which is lower than some other reported results (Di et al., 2005; Jia et al., 2002; Xiao et al., 2000.). In addition, the sensor reached 95% of the steady-state current within 6 s, which allowed the convenient quantification of H_2O_2.

The Lineweaver–Burk form of the Michaelis–Menten equation is $1/i_{ss} = 1/i_{max} + K_m^{app}/(ci_{max})$, where i_{ss} is the steady-state current after the addition of substrate, i_{max} is the maximum current under saturated substrate conditions, and c in μM is the concentration of substrate (H_2O_2), the K_m^{app} is the Michaelis–Menten constant. By drawing a plot of $1/i_{ss}$ versus $1/c$, we obtained a linearly regressed slope value of 6.46 μM μA^{-1} and an intercept value of 0.00160 μA^{-1}, with a linearity correlation coefficient of 0.999. Thus, the value of K_m^{app} is calculated to be 4.04 mM.

3.5. Reproducibility and stability

The repeatability of one enzyme electrode was examined in the presence of 0.500 mM H_2O_2 in 50.0 mM PBS (pH 7.0). The relative standard deviation was 3.1% for eight successive assays. The storage stability of one enzyme electrode was studied over a period of 20 days. By storing it as a dry film in the refrigerator at 4 °C and measuring once a day, the biosensor performed well in 15 days, since the response current for 0.500 mM H_2O_2 decreased by about 5%, as shown in Fig. 3S in the Supplementary Data.

4. Conclusions

In summary, we have developed and characterized a new third-generation H_2O_2 biosensor based on its reduction reaction

catalyzed by HRP immobilized on a gold electrode coated with a new nanocomposite film of TTF–TCNQ/MWCNTs. The adsorption of MWCNTs on the electrode surface improved the growth of tress-like TTF–TCNQ crystals for the direct electron communication between the active center of HRP and the electrode. The fabricated H_2O_2 biosensor exhibited good performance for H_2O_2 assay at 0 V. A simple and novel EQCM method has been proposed to evaluate the ESA of the immobilized HRP. It is expected that other similar CTC-based nanocomposites find wide biosensing applications in the future.

Acknowledgements

This work was supported by the National Natural Science Foundation of China (20675029, 90713018, 20335020), the Basic Research Special Program of the Ministry of Science and Technology of China (2003CCC00700), the Foundation of the Ministry of Education (MOE) of China and Hunan Provincial Education Department (04C383, 05A036), and the State Key Laboratory of Electroanalytical Chemistry. Cao and Jiang contributed equally to this work.

Appendix A. Supplementary data

Supplementary data associated with this article can be found, in the online version, at doi:10.1016/j.bios.2008.03.021.

References

Albery, W.J., Bartlett, P.N., Bycroft, M., Craston, D.H., Briscol, B.J., 1987. J. Electroanal. Chem. 218 (1–2), 119–126.
Albery, W.J., Bartlett, P.N., Craston, D.H., 1985. J. Electroanal. Chem. 194 (2), 223–235.
Bartlett, P.N., Ali, Z., Eastwickfield, V., 1992. J. Chem. Soc. Faraday Trans. 88 (18), 2677–2683.
Bartlett, P.N., Tong, X.Q., 1997. J. Phys. Chem. B 101 (42), 8540–8549.
Buttry, D.A., Ward, M.D., 1992. Chem. Rev. 92 (6), 1355–1379.
Cenas, N.K., Kulys, J.J., 1981. Bioelectrochem. Bienergy 8 (1), 103–113.
Chen, H., Dong, S., 2007. Biosens. Bioelectron. 22 (8), 1811–1815.
Decker, L.A., 1977. Worthington: Worthington Biochemical Corporation, Worthington Enzyme Manual. Freehold, New Jersey.
Di, J.W., Bi, S.P., Zhang, M., 2004. Biosens. Bioelectron. 19 (11), 1479–1486.
Di, J.W., Shen, C.P., Peng, S.H., Tu, Y.F., Li, S.J., 2005. Anal. Chim. Acta 553, 196–200.
Freund, M.S., Brajter-Toth, A., 1989. Anal. Chem. 61 (9), 1048–1052.
Freund, M.S., Brajter-Toth, A., Ward, M.D., 1990. J. Electroanal. Chem. 289 (1–2), 127–141.
Gorton, L., Jonsson-Peterson, G., Csoregi, E., Johansson, K., Dominguez, E., Marko-Varga, G., 1992. Analyst 117, 1235–1241.
Heller, A., 1992. J. Phys. Chem. 96 (9), 3579–3587.
Hill, B.S., Scolari, C.A., Wilson, G.S., 1988. J. Electroanal. Chem. 252 (1), 125–138.
Jaeger, C.D., Bard, A.J., 1979. J. Am. Chem. Soc. 101 (7), 1690–1699.
Jaeger, C.D., Bard, A.J., 1980. J. Am. Chem. Soc. 102 (17), 5435–5442.
Jia, J., Wang, B., Wu, A., Cheng, G., Li, Z., Dong, S., 2002. Anal. Chem. 74, 2217–2223.
Kang, X., Mai, Z., Zou, X., Cai, P., Mo, J., 2007. Anal. Biochem. 369 (1), 71–79.
Khan, G.F., Ohwa, M., Wernet, W., 1996. Anal. Chem. 68 (17), 2939–2945.
Khan, G.F., Kobatake, E., Shinohara, H.S., Ikariyama, Y., Aizawa, M., 1992. Anal. Chem. 64 (11), 1254–1258.
Koopal, C.G.J., Feiters, M.C., Nolte, R.J.M., Deruiter, B., Schasfoort, R.B.M., Czajka, R., Vankempen, H., 1992. Synth. Met. 51 (1–3), 397–405.
Korell, U., Spichiger, U.E., 1993. Electroanalysis 5 (9–10), 869–876.
Korell, U., Spichiger, U.E., 1994. Anal. Chem. 66 (4), 510–515.
Luo, X., Killard, A.J., Morrin, A., Smyth, M.R., 2006. Anal. Chim. Acta 575 (1), 39–44.
Os, P.J.H.J. van, Bult, A., Koopal, C.G.J., Bennekom, W.P. van, 1996. Anal. Chim. Acta 335 (3), 209–216.
Palmisano, F., Zambonin, P.G., Centonze, D., Quinto, M., 2002. Anal. Chem. 74 (23), 5913–5918.
Qian, L., Yang, X., 2006. Talanta 68 (3), 721–727.
Razola, S.S., Ruiz, B.L., Diez, N.M., Mark Jr., H.B., Kauffmann, J.M., 2002. Biosens. Bioelectron. 17 (11–12), 921–928.
Ren, C.B., Song, Y.H., Li, Z., Zhu, G.Y., 2005. Anal. Bioanal. Chem. 381 (6), 1179–1185.
Song, Y.H., Wang, L., Ren, C.B., Zhu, G.Y., Li, Z., 2006. Sens. Actuators B 114 (2), 1001–1006.
Stoica, L., Ludwig, R., Haltrich, D., Gorton, L., 2006. Anal. Chem. 78 (2), 393–398.
Su, Y., Xie, Q., Chen, C., Zhang, Q., Ma, M., Yao, S., 2008. Biotechnol. Prog. 24 (1), 262–272.
Tang, M.Y., Yuan, R., Chai, Y.Q., 2006. Chin. J. Chem. 24 (11), 1575–1580.
Wang, J., 2008. Chem. Rev. 108, 814–825.
Xiao, Y., Ju, H.X., Chen, H.Y., 2000. Anal. Biochem. 278 (1), 22–28.
Xu, S.Y., Han, X.Z., 2004. Biosens. Bioelectron. 19 (9), 1117–1120.
Yabuki, S., Shinohara, H., Aizawa, M., 1989. Chem. Commun., 49–50.
Zhao, G., Feng, J.J., Xu, J.J., Chen, H.Y., 2005. Electrochem. Commun. 7 (7), 724–729.
Zhou, A., Xie, Q., Yuan, Y., Zhang, Y., Yao, S., 2000. Anal. Chim. Acta 419 (2), 251–254.
Zhou, Q., Xie, Q., Fu, Y., Su, Z., Jia, X., Yao, S., 2007. J. Phys. Chem. B 111 (38), 11276–11284.